

## Article

# Mechanical Strengths of Alkali-Activated Blast Furnace Slag Powder with Different Alkali Activators and Plant Fibers

Jing Zhu <sup>1,\*</sup>, Lizhuo Song <sup>1</sup>, Zijian Qu <sup>1</sup>, Xiaopeng Wang <sup>1</sup>, Zijie Wen <sup>1</sup> , Xiaodong Liu <sup>2,\*</sup> and Hui Wang <sup>3,\*</sup>

<sup>1</sup> College of Civil Engineering and Architecture, Harbin University of Science and Technology, Harbin 150080, China; songlizhuo12@163.com (L.S.); 1715020417@stu.hrbust.edu.cn (Z.Q.); m13048993423@163.com (Z.W.)

<sup>2</sup> School of Energy and Built Environment, Guilin University of Aerospace Technology, Guilin 541004, China

<sup>3</sup> School of Civil and Environmental Engineering, Ningbo University, Ningbo 315000, China

\* Correspondence: zhujing@hrbust.edu.cn (J.Z.); liuxd@hrbust.edu.cn (X.L.); wanghui4@nbu.edu.cn (H.W.)

**Abstract:** In this paper, the influence of water glass types, the modulus of water glass, the alkali content, the water consumption, and plant fibers on the mechanical strengths of alkali-activated blast furnace slag powder (BFS) is investigated. Moreover, the fiber types and pretreatment on the plant fibers and the measuring temperature on the performance of alkali-activated BFS are further considered. Results indicate that BFS activated by potassium silicate shows higher mechanical strengths than that activated by sodium silicate. The alkali-activated BFS with alkali treatment on fibers is the most advantageous. The modulus of alkali leads to decreasing the compressive strength. A total of 35% water consumption is the most beneficial to the specimens' flexural and compressive strengths. Samples with 14% potassium silicate show the maximum mechanical strength. Alkali-activated BFS with 1% wheat straw fibers in addition by total volume represents the maximum mechanical strength. The alkali-activated BFS with alkali treatment on fibers is the most advantageous. The addition of potassium silicate can improve the flexural and compressive strengths by the maximum values of 30.4% and 16.8% compared to specimens with sodium silicate. A total of 35% water consumption can increase the flexural and compressive strengths by 33.8% and 32.7%.

**Keywords:** water glass; alkali-activated; blast furnace slag powder; mechanical strengths; potassium silicate



**Citation:** Zhu, J.; Song, L.; Qu, Z.; Wang, X.; Wen, Z.; Liu, X.; Wang, H. Mechanical Strengths of Alkali-Activated Blast Furnace Slag Powder with Different Alkali Activators and Plant Fibers. *Coatings* **2023**, *13*, 664. <https://doi.org/10.3390/coatings13030664>

Academic Editor: Valeria Vignali

Received: 10 March 2023

Revised: 19 March 2023

Accepted: 20 March 2023

Published: 22 March 2023



**Copyright:** © 2023 by the authors. Licensee MDPI, Basel, Switzerland. This article is an open access article distributed under the terms and conditions of the Creative Commons Attribution (CC BY) license (<https://creativecommons.org/licenses/by/4.0/>).

## 1. Introduction

Ordinary Portland Cement (OPC) is one of the most widely used cement-based building materials, which is consumed a lot in engineering construction [1]. The annual CO<sub>2</sub>, SO<sub>2</sub>, and NO<sub>x</sub> emissions from OPC production around the world account for about 8% of the global CO<sub>2</sub> emissions [2]. During the entire production process of OPC, approximately 3.2 GJ (gigajoule) per ton is consumed [3–7]. The residual energy and hazardous gas can accelerate the greenhouse effect. In order to postpone the acceleration, some new energy-saving and environmentally protected cementitious materials need to be developed.

In recent years, fly ash, slag powder, and volcanic ash are used as cementitious materials in concrete [8–16]. These mineral admixtures can improve the mechanical strengths when the curing temperature is higher than 40 °C and the curing age is higher than 28 days [17]. However, when the curing temperature and the curing age are lower than 40 °C and 28 days, respectively, the mechanical strengths are decreased by the addition of mineral admixtures [18]. The alkali slag cement-based material has become a popular green and environmentally friendly material studied at home and abroad [19,20]. This kind of material shows excellent mechanical strengths when cured in several curing environments and curing ages [21,22]. Prior researchers have developed alkali-activated mineral admixtures with ultra-high mechanical strengths. As pointed out by prior researchers, the mechanical performance of alkali-activated blast furnace slag (BFS) shows higher mechanical strength

and durability than the alkali-activated fly ash [23–27]. Therefore, in this paper, the BFS is applied in manufacturing the alkali-activated binder materials and the corresponding properties should be intensively studied. In previous studies, sodium silicate is a common activator in the alkali-activated cementitious materials. However, little attention has been paid to the influence of types of activators on the properties of alkali-activated cementitious materials [28,29].

Micro-fine steel fibers have been used for reinforcing the mechanical strengths of alkali-activated BFS by prior researchers. However, most of the steel fibers sink to the bottom of the samples during manufacture, leading to the uneven distribution of steel fibers [30]. Mastali et al. [31] have reported that the polyvinyl alcohol fibers, basalt fibers, and polypropylene fibers can improve the mechanical strengths of alkali-activated BFS, but the corresponding heat resistance is poor.

Plant fibers can not only significantly improve the toughness of the matrix material, inhibit the shrinkage of the material, and limit the crack propagation, but also make a large use of industrial and agricultural wastes such as slag and wheat straw to recycle resources [32]. As obtained in Zhu's research, alkali-activated BFS with plant fibers shows excellent heat resistance [33]. Although multiple performances of alkali-activated mineral admixtures have been studied by several scholars [34–36], little attention has been paid to the types of silicate, the type, dosages, and treatment methods of reinforced fibers.

In this study, the influence of silicate types and contents, the fibers' volume, and the effects of the fibers' type on the flexural and compressive strength of alkali-activated BFS are investigated. Moreover, the treatment method of the fibers and the modulus of the silicate are considered. The scanning electron microscope is used for revealing the inner mechanism of the mechanical properties. This research will provide a reference for developing alkali-activated mineral admixtures with excellent mechanical performance and durability in the future. As an inorganic adhesive, the alkali-activated BFS can be used in the repair of road, beam, and column in the future.

## 2. Experimental

### 2.1. Raw Materials

The alkali-activated BFS powder in our study is composed of the BFS powder, sodium silicate ( $\text{Na}_2\text{O}\cdot n\text{SiO}_2$ ), potassium silicate ( $\text{K}_2\text{O}\cdot n\text{SiO}_2$ ), sodium hydroxide (NaOH), and water. Potassium silicate ( $\text{K}_2\text{O}\cdot n\text{SiO}_2$ ) and sodium silicate ( $\text{Na}_2\text{O}\cdot n\text{SiO}_2$ ) are provided by Huida Chemical Plant (Tianjin, China). The baume degree, initial modulus, and density of potassium silicate are 46.3, 2.76, and  $1.465\text{ g/cm}^3$ , respectively. The content of  $\text{SiO}_2$  and  $\text{K}_2\text{O}$  of potassium water glass are 28.15% and 15.98%, respectively. Sodium silicate shows the baume degree, initial modulus, and density of 48.0, 2.3, and  $1.495\text{ g/cm}^3$ , respectively. At the same time, the corresponding  $\text{SiO}_2$  and  $\text{K}_2\text{O}$  of sodium water glass are 31.10% and 13.51%, respectively. NaOH is provided by Harbin Chemical Reagent Factory (Harbin, China), with the purity of 99.3%.

NaOH and KOH are provided by Harbin Chemical Reagent Factory (Harbin, China), with the purity of 99.4% and 99.1%, respectively.

The wheat straw fibers, rice straw fibers, and corn straw fibers are produced by Anshan Changhong Fiber Factory (Anshan, China). The diameters of the fibers are 5, 3, and 7 mm, while the lengths of the fibers are 3, 2.5, and 2 cm showing the aspect ratios of 18, 16.7, and 11.4, respectively. The densities of the fibers are 1.55, 1.0, and  $0.25\text{ g/cm}^3$ , with the tensile strength of the fibers being 20, 8, and 12 MPa, respectively.

Polypropylene fibers (PP)s produced by Shandong Senhong Co., Ltd. (Taian, China) have a diameter of 18–45  $\mu\text{m}$ , an average length of 12 mm, and show an aspect ratio of 267. The density, the elastic modulus, and the tensile strength of PPs are  $0.91\text{ g/cm}^3$ , 42 GPa, and 1600 MPa, respectively. Micro-steel fibers (MS) produced by Anshan Changhong Steel Fiber Factory (Anshan, China) show a diameter of 0.22 mm, a length of 13 mm, and perform an aspect ratio of 59.1. Additionally, the density and tensile strength of MS are  $7.8\text{ g/cm}^3$  and 2870 MPa, respectively. Coarse steel fibers (CS) produced by Huaixing Steel Fiber

Processing Plant in Taocheng District of Hengshui City ( Hengshui, China) have a diameter of 2.5 mm and a length of 2~3 cm. At the same time, the aspect ratio, the density, and the tensile strength of CS are 10, 7.8 g/cm<sup>3</sup>, and higher than 2150 MPa, respectively. The morphology of fibers is shown in Figure 1. The technical indicators of applied fibers are measured and provided by the manufacturers.

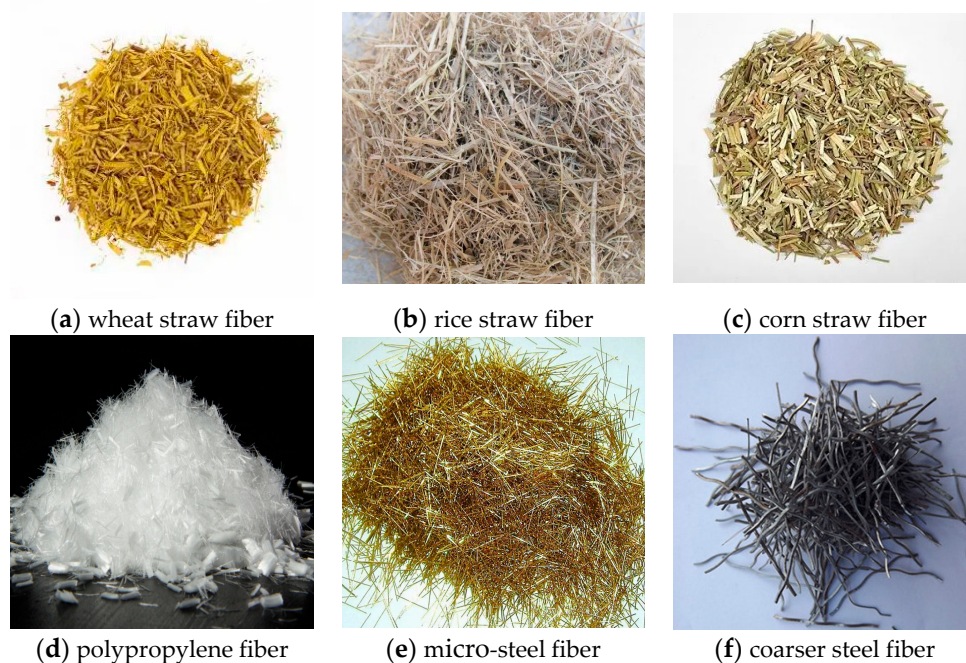


**Figure 1.** The fibers used in alkali-activated BFS.

The S95 BFS powder with specific surface area of 475 m<sup>2</sup>/kg is provided by Liaoyuan Jingang Company (Liaoyuan, China). The main activity indicators, the mass coefficient, alkaline coefficient, and activity coefficient of BFS powder are 1.91, 1.03, and 0.44, respectively. The main chemical components of raw materials are shown in Table 1.

**Table 1.** Main chemical composition of BFS (%).

Types	SiO <sub>2</sub>	Al <sub>2</sub> O <sub>3</sub>	CaO	MgO	Fe <sub>2</sub> O <sub>3</sub>	TiO <sub>2</sub>	MnO	K <sub>2</sub> O
BFS	36.9	15.66	37.57	9.3	0.36	0.18	0.16	0.25

## 2.2. Specimens' Preparation

The mass ratios of potassium silicate used in this study are 11.7%, 12.7%, 14.1%, 15.8%, 16.9%, and 17.8% by the total mass of alkali-activated BFS (see Table 2). At the same time, the corresponding mass ratios of NaOH are 3.9%, 3.1%, 2.5%, 1.6%, 0.9%, and 0.4%, respectively. First, NaOH is slowly poured into the water glass and stirred with a glass rod until there are no obvious floccules. The mixture is allowed to stand for 1.5 h until the heat release is finished. After that, the BFS powder and fibers are added to the cement slurry mixer, and the water glass with adjusted modulus is added to the mixer and stirred at the speed of 140 r/min for 1 min. Then, the weighted water is added to the mixer and stirred at the same stirring speed for 6 min. When the mixing is finished, the mixture is poured into steel molds of sizes 40 mm × 40 mm × 160 mm and 100 mm × 100 mm × 100 mm, and then all specimens are formed by high-frequency vibration on the concrete vibration table. The specimens are cured in a room with 20 ± 1 °C and relative humidity of 52.1% for 24 h. Finally, all samples are moved to a standard curing room with a relative humidity of 98.1% and a temperature of 20 ± 2 °C for the curing ages of 3, 7, and 28 days. The experimental details can be found in Feng's research [37].

**Table 2.** The mixing proportions of alkali-activated BFS powder.

Modulus	Alkali Content (%)	BFS (kg)	Water Glass Types	Water Glass (kg)	NaOH (kg)	Water–Binder Ratio	Fiber Types	Fiber Volume (%)	Fiber Treatment Method
1.0	14	1562.5	Potassium	339.6	84.2	32	-	-	-
1.0	14	1562.5	Sodium	393	97.3	32	-	-	-
0.8	12	1562.5	Potassium	267.7	89.2	35	-	-	-
1.0	12	1562.5	Potassium	291	72.1	35	-	-	-
1.2	12	1562.5	Potassium	323.7	57.2	35	-	-	-
1.6	12	1562.5	Potassium	361.7	35.7	35	-	-	-
2.0	12	1562.5	Potassium	388.9	21.1	35	-	-	-
2.4	12	1562.5	Potassium	409.5	8.3	35	-	-	-
1.0	8	1562.5	Potassium	199.1	47.7	35	-	-	-
1.0	10	1562.5	Potassium	248.8	59.6	35	-	-	-
1.0	12	1562.5	Potassium	291	72.1	35	-	-	-
1.0	14	1562.5	Potassium	348.4	83.4	35	-	-	-
1.0	16	1562.5	Potassium	398.2	95.3	35	-	-	-
1.0	18	1562.5	Potassium	447.9	107.2	35	-	-	-
1.0	20	1562.5	Potassium	497.7	241.2	35	-	-	-
1.0	22	1562.5	Potassium	547.5	131.1	35	-	-	-
1.0	12	1562.5	Potassium	291	72.1	28	-	-	-
1.0	12	1562.5	Potassium	291	72.1	32	-	-	-
1.0	12	1562.5	Potassium	291	72.1	35	-	-	-
1.0	12	1562.5	Potassium	291	72.1	38	-	-	-
1.0	12	1562.5	Potassium	291	72.1	42	-	-	-
1.0	12	1562.5	Potassium	291	72.1	35	Wheat straw	1	-
1.0	12	1562.5	Potassium	291	72.1	35	Rice	1	-
1.0	12	1562.5	Potassium	291	72.1	35	Corn	1	-
1.0	12	1562.5	Potassium	291	72.1	35	PP	1	-
1.0	12	1562.5	Potassium	291	72.1	35	XS	1	-
1.0	12	1562.5	Potassium	291	72.1	35	CS	1	-
1.0	12	1562.5	Potassium	291	72.1	35	Wheat	1	Acid
1.0	12	1562.5	Potassium	291	72.1	35	Wheat	1	Acid
1.0	12	1562.5	Potassium	291	72.1	35	Wheat	1	Alkali
1.0	12	1562.5	Potassium	291	72.1	35	Wheat	1	Alkali
1.0	12	1562.5	Potassium	291	72.1	35	Wheat	1	-
1.0	12	1562.5	Potassium	291	72.1	35	Wheat	0.2	Alkali
1.0	12	1562.5	Potassium	291	72.1	35	Wheat	1	Alkali
1.0	12	1562.5	Potassium	291	72.1	35	Wheat	3	Alkali
1.0	12	1562.5	Potassium	291	72.1	35	Wheat	5	Alkali

The treatment method on the plant fibers is described as follows. The sulfuric acid treatment and hydrochloric acid treatment are provided. The fibers are immersed in 10% sulfuric acid solution or hydrochloric acid solution for 60 min, and then the fibers are treated in deionized water for 2 min. After all these are finished, the treated plant fiber is dried naturally in a cool place. The fibers with alkali treatment are shown as follows. The plant fibers are immersed in 10% NaOH solution for 60 min, and then are moved in water for 2 min.

### 2.3. Measurement Methods

#### Measurement of Mechanical Strength

The YAW-300 cement flexural and compressive constant stress testing machine produced by Beijing Longchen Weiye (Beijing, China), is used for the measurement of mechanical strengths. The maximum compressive strength and flexural strength were 300 and 10 KN, respectively. The measurement accuracy ranges from 1% to 100%. The loading speeds for the compressive and flexural strengths are 2.4 and 0.05 kN/s, respectively. First, the mortar specimen is placed on the YAW-300 automatic compression-folding testing

machine and folded into two halves. Then, half of the fractured prism specimen is placed in the middle of the compressive clamp, and the compression surface is the two sides of the specimen during forming. The mechanical strengths of alkali-activated BFS are measured in accordance with Chinese standard GB/T 17671-2021 [38]. The measuring process is shown in Figure 2.



Flexural strength measurement

Compressive strength measurement

**Figure 2.** Measurement of mechanical strengths.

#### 2.4. Steps of Micro-Performance

The central crushing part of the sample is selected for scanning electron microscope (SEM) measurement. The fragments are cut into small particles of about 5 mm, regular shape and smooth surface by pliers. On a fixed metal plate, the sample is fixed with conductive adhesive and vacuumed in a vacuum machine. After this, the samples are used to obtain photographs of the scanning electron microscope by the FEI Sirion model scanning electron microscope which is provided by Philips of Amsterdam, The Netherlands. Instrument resolution is demonstrated by the following: when the voltage > 10 kV, 1.5 nm; when the voltage is 1 kV, 2.5 nm; and when the voltage is 500 kV, 3.5 nm. The acceleration voltage is 200 V~30 kV, the sample chamber diameter is 284 mm, and the analysis working distance is 5 mm. This measurement is carried out following GB/T 17362-2008 [39]. Figure 3 shows the measuring process of the SEM. Table 3 shows the test device specifications and standards corresponding to different experiments.

**Table 3.** The test device specifications and standards corresponding to different experiments.

Parameter	Mechanical Strength	Micro-Performance
Equipment	YAW-300	FEI Sirion
Specification	Flexural strength: 0~10 KN Compressive strength: 0~300 KN	Magnification: 74×~300,000×
Manufacturer	Beijing Longchen Weiye, Beijing, China	Philips of The Netherlands
Standard	GB/T 17671-2021	GB/T 17362-2008

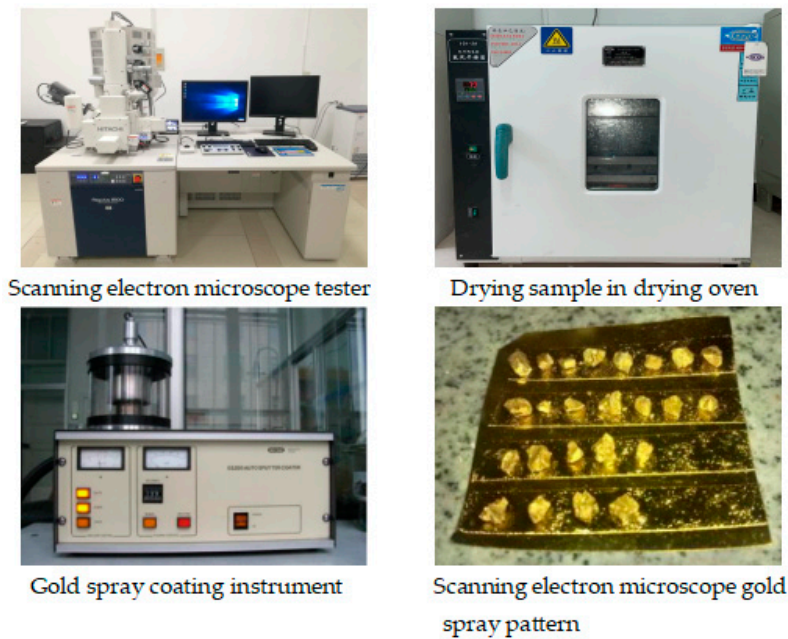


Figure 3. Measurement of SEM.

### 3. Results and Discussion

#### 3.1. Influence of Silicate Type

Potassium silicate and sodium silicate are used as alkali activators to excite BFS. The flexural strength and compressive strength of the specimens are measured after standard cured for 3, 7, and 28 days. The measuring results are illustrated in Figure 4. As shown in Figure 4, the flexural strengths of the specimen mixed with potassium silicate are 3%, 24%, and 30.4% higher than that of the specimen mixed with sodium silicate. The compressive strength of the specimens mixed with potassium silicate cured for 3, 7, and 28 days is 4.4%, 3.3%, and 16.8% higher than that of the specimens mixed with sodium silicate. It is obvious that potassium silicate is superior to sodium silicate in strengthening the mechanical properties of the alkali-activated BFS [40,41]. When the amount of sodium silicate is small, the reaction and the potential activity of slag cannot be thoroughly and fully excited. Excessive dosage of sodium silicate will lead to a high concentration of  $\text{OH}^-$  ions, and the hydration products generated by the rapid reaction on the surface of slag particles form a protective film, which prevents the further progress of the reaction and leads to slow development of the strength in the later stage [42]. In the follow-up experimental results, potassium water glass is selected as alkali activator.

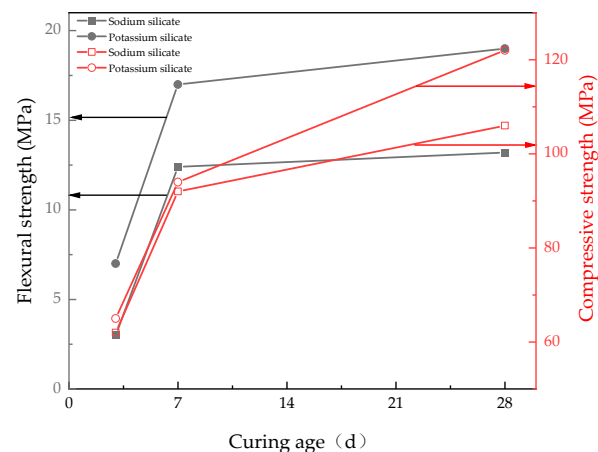
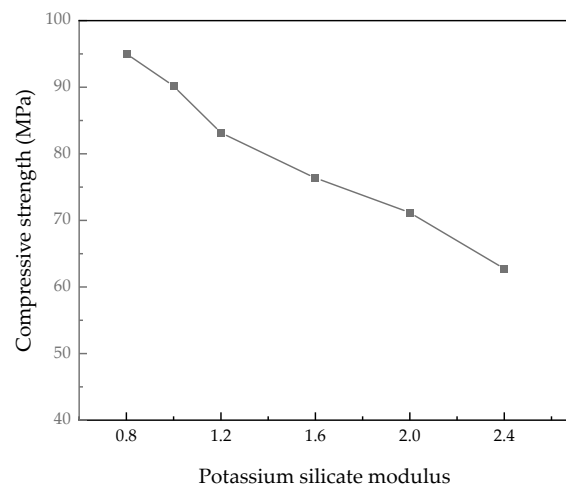


Figure 4. The mechanical strengths of alkali-activated BFS with different alkali activators.

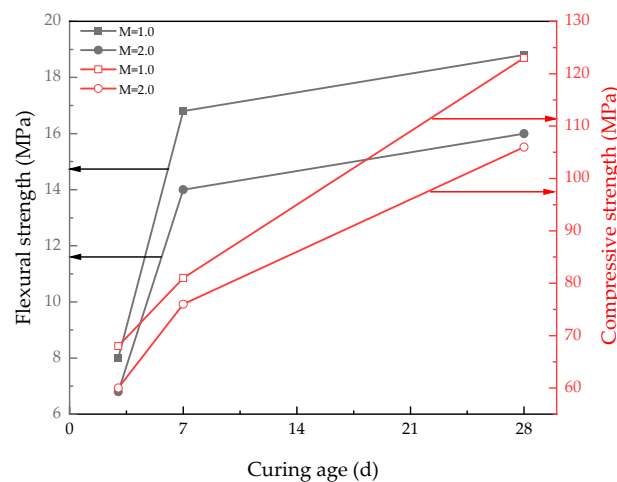
### 3.2. Influence of Modulus

As reported in prior research, unreasonable water consumption will bring inconvenience to the construction of alkali-activated BFS. According to prior research [43], the modulus 0.8~2.4 is reasonable to the mechanical properties of alkali-activated BFS. Therefore, in this study, this modulus range is taken as the potassium silicate, and the compressive strength of specimens is determined. The compressive strength of the specimens cured in the standard environment for 28 days is shown in Figure 5. The compressive strength decreases with the increasing modulus. The compressive strength of specimens with the modulus of 0.8 is 53% higher than the specimens with the modulus of 2.4. This is ascribed to the fact that when the modulus increases, the alkali solution can not be able to fully activate the slag activity due to insufficient alkalinity, resulting in the reduction of compressive strength [44].



**Figure 5.** The compressive strength of alkali-activated BFS with different modulus.

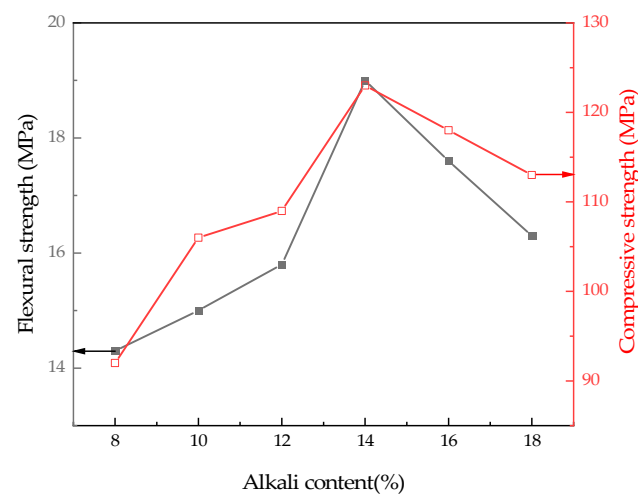
Figure 6 shows the flexural and compressive strengths of potassium silicate with modulus of 1.0 and 2.0. The curing age ranges from 3 to 28 days. As depicted in Figure 6, the flexural strengths of the specimens with modulus of 1.0 cured for 3, 7, and 28 days are 24.2%, 14.6%, and 15.9% higher than that of the specimen whose modulus is 2.0. Moreover, as illustrated in Figure 6, specimens with modulus of 1.0 cured for 3, 7, and 28 days show the compressive strength 10.1%, 27.1%, and 12.9% higher than that of the specimen with modulus of 2.0. This is due to the improved hydration degree by the increased curing age [45].



**Figure 6.** Mechanical strengths of alkali-activated BFS with different curing age and modulus.

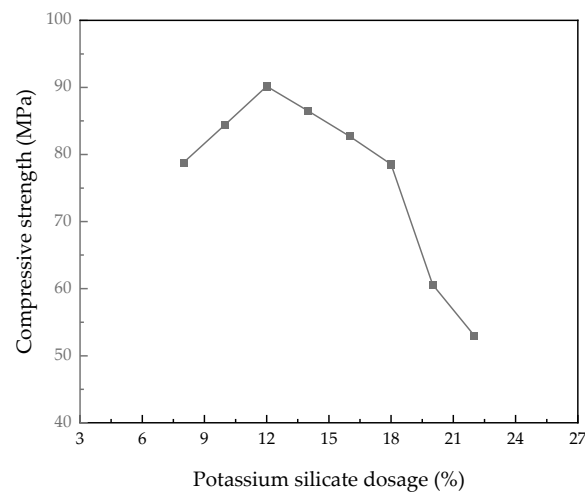
### 3.3. Effect of Alkali Content

Figure 7 shows the flexural and compressive strengths of potassium silicate with different dosages of alkali. As found in Figure 7, the flexural strength and compressive strengths of the specimens with 14% alkali are 33.8% and 32.7% higher than those with 8% alkali. Meanwhile, the flexural strength and compressive strength of the specimens with 14% alkali are 21.2% and 17.1% higher than those with 18% alkali content. Additionally, the flexural strength and compressive strength of the specimens with 14% alkali content are 20.3% and 11.9% higher than those with 12% alkali. This is because the alkali is beneficial in stimulating the activity of slag, enhancing the dissolution and recombination ability of slag, forming more calcium silicate hydrate gel, and filling some pores' inner specimens. Therefore, the mechanical strengths are improved. When the alkali content is 14%, the alkali solution is sufficient to stimulate the activity of slag. However, with the continuous increase of alkali content, the production of calcium silicate hydrate gel will be inhibited, leading to the increase of the number and sizes of pores, thus decreasing the mechanical strength.



**Figure 7.** Mechanical strengths of alkali-activated BFS with different alkali contents.

The compressive strength of alkali-activated BFS with different dosages of potassium silicate is shown in Figure 8. As illustrated in Figure 8, the compressive strength of alkali-activated BFS first increases and then decreases with the increasing dosages of potassium silicate. The compressive strength reaches the maximum value when the dosage of potassium silicate is 12%. This can be ascribed to the reason that a small amount of potassium silicate will lead to an incomplete reaction and the potential activity of BFS can not be fully activated in the process of hydration [46,47]. Therefore, the compressive strength is increased by the addition of potassium silicate, when the amount ranges from 8% to 12%. However, when the amount of potassium silicate increases from 12% to 22%, the compressive strength decreases. The maximum value of compressive strength of the specimens with 12% potassium silicate is 1.7 multiples of the specimens with 22% potassium silicate. This is ascribed to the fact that with the increasing dosage of potassium silicate, the activity of BFS is improved by adding more potassium silicate. However, when the dosage is higher than 12%, because the excessive alkali reacts with  $\text{CO}_2$ , forming carbonates on the surface of hydration, this prevents a further reaction. Consequently, the mechanical strengths decrease with the dosage of potassium silicate ranging from 12% to 22%.



**Figure 8.** The compressive strength of alkali-activated BFS with different potassium silicate.

### 3.4. Effect of Water Consumption

Figure 9 shows the mechanical strengths of alkali-activated BFS with water consumption increasing from 28% to 42%. As demonstrated in Figure 9, the flexural and compressive strengths of alkali-activated BFS with 35% water consumption reach the highest, while specimens with 42% water consumption show the lowest mechanical strengths. The flexural and compressive strengths of specimens with water consumption of 35% are 313% and 35.5% of the specimens with 42% water consumption. This is ascribed to the fact that the addition of deionized water can increase fluidity of fresh alkali-activated BFS, leading to increasing the transport of free alkali ions. More silicon oxide tetrahedron and aluminum oxide tetrahedron formed, resulting in increasing the mechanical strengths. However, the volume and quantity of pores' inner alkali-activated BFS are increased by excessive water, which decreases the mechanical strengths [48].

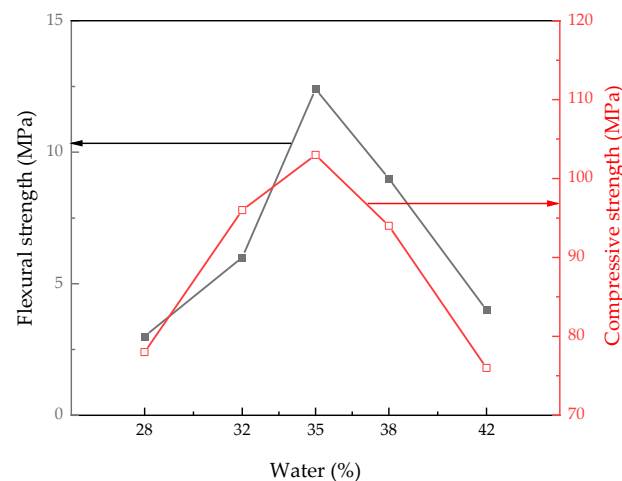


**Figure 9.** The mechanical strengths of alkali-activated BFS with different potassium silicate.

### 3.5. Effect of Plant Fiber Types

Figure 10a shows the mechanical strengths of alkali-activated BFS with wheat straw fibers, rice straw fibers, or corn straw fibers. As illustrated in Figure 10a, the mechanical strengths increase with the rising curing ages due to the increased hydration degree by curing age. The mechanical strengths of the specimens decrease in this order: alkali-activated BFS with wheat straw > alkali-activated BFS with corn straw > alkali-activated BFS without fiber > alkali-activated BFS with rice straw fibers. This is because the wheat straw is well occluded with the substrate, which enhances the contact interface between

fibers and the alkali-activated BFS matrix [49]. However, the density of corn stalk is lower than the alkali-activated BFS matrix; therefore, the corn stalk floats on the surface of alkali-activated BFS. Consequently, alkali-activated BFS with corn stalk shows the worst mechanical strengths.

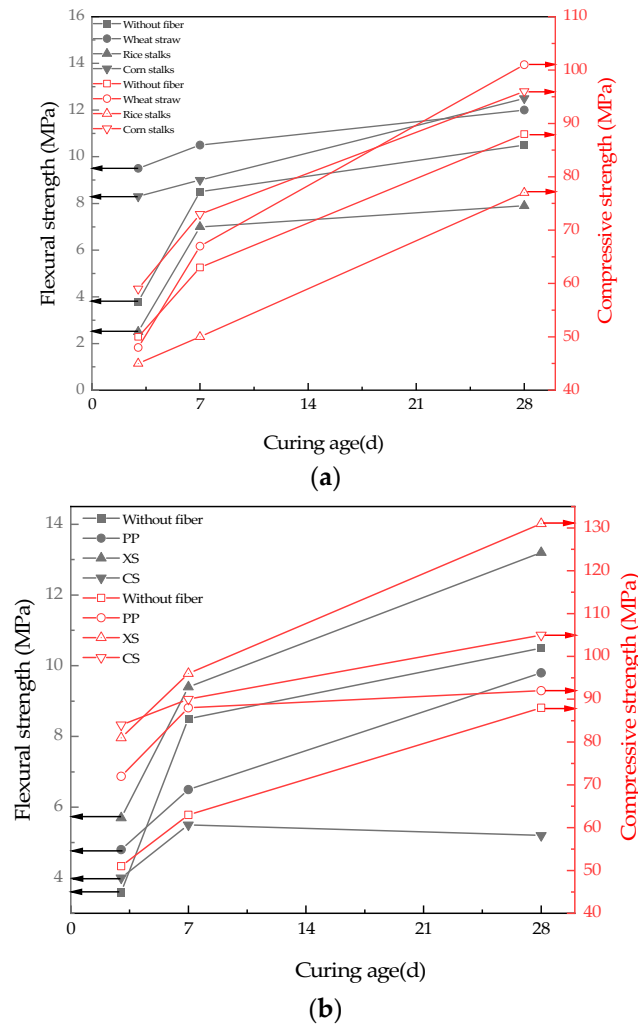


**Figure 10.** Mechanical strengths of alkali-activated BFS with different fibers. (a) Plant fibers; (b) Polypropylene fiber (PP), fine steel fiber (XS), and coarser steel fiber (CS).

Figure 10b shows the mechanical strengths of alkali-activated BFS with PP, XS, or CS fibers. As illustrated in Figure 10b, the mechanical strengths increase with the rising curing ages due to the increased hydration degree by curing age. The mechanical strengths of the specimens decrease in this order: alkali-activated BFS with XS > alkali-activated BFS with CS > alkali-activated BFS with PP > alkali-activated BFS without fiber. XS and CS have higher mechanical strength than wheat straw. However, due to their high density and heavy mass, most of the steel fibers sink to the bottom of the specimen during the coagulation process of alkali-activated BFS. The distribution is uneven, resulting in great differences in the specimens.

### 3.6. Effects of Different Treatment Methods on Plant Fiber

The mechanical strengths of alkali-activated BFS with different treatment methods on the plant fibers are shown in Figure 11. As observed in Figure 11, the mechanical strengths show an ascending trend with the increasing curing age due to the increased hydration degree. The mechanical strengths of alkali-activated BFS with different treatment

methods on the plant fibers show the order of alkali-activated BFS with alkali treatment > alkali-activated BFS with acid treatment > alkali-activated BFS without any treatment. This is attributed to the fact that alkali treatment and acid treatment can improve the bonding performance of fibers and alkali-activated BFS, leading to improve the mechanical strengths [50]. Moreover, the alkali treatment and acid treatment lead to improving the dispersing degree of fibers and enhancing the mechanical strengths of alkali-activated BFS. In addition, the dispersing effect of alkali treatment on fibers is higher than the acid treatment, resulting in increasing the mechanical strength [51].

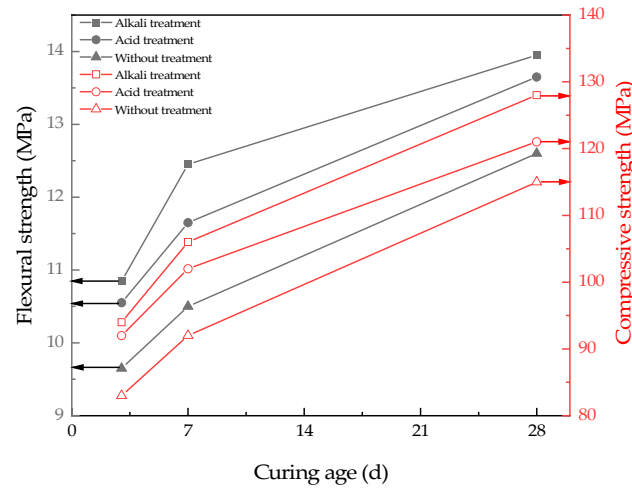


Figure 11. Mechanical strengths of alkali-activated BFS with different treatment methods.

3.7. Effects of Plant Fiber Content

Figure 12 shows the mechanical strengths of alkali-activated BFS with wheat straw. The wheat straw is treated by alkali and the specimens are cured in the standard environment for 28 days. As depicted in Figure 12, the specimens with 1% fibers show the maximum flexural and compressive strengths. When the volume ratio of fibers increases from 0.2% to 1%, the flexural and compressive strengths increase by 26.9% and 16.3%, respectively. Meanwhile, when the volume ratio of fibers ranges from 1% to 5%, the flexural and compressive strengths increase by 58.3% and 66.1% respectively. This is ascribed to the fact that when the volume of fibers is less than 1%, the increasing dosages of fibers can effectively improve mechanical strength by bridging the inner cracks. However, excessive fibers can agglomerate, leading to decreasing the mechanical strengths [52,53].

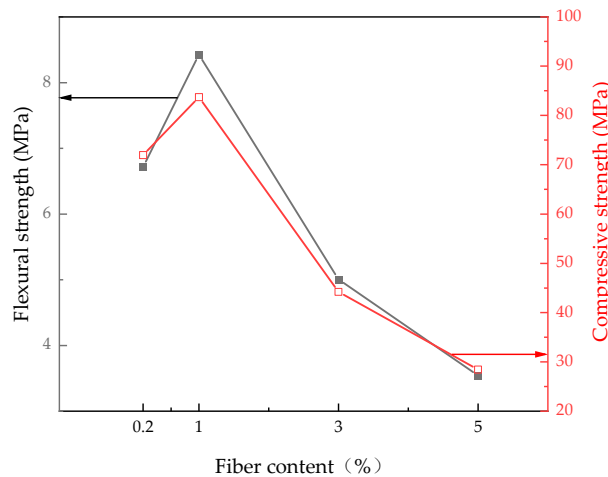


Figure 12. Mechanical strengths of alkali-activated BFS with different dosages of fibers.

### 3.8. Scanning Electron Microscope

Figure 13 shows the alkali-activated BFS with 1% wheat straw fibers, rice straw fibers, and corn stalk fibers, respectively. As illustrated in Figure 13a, strip substance can be found in the SEM photos of specimens with wheat straw fibers. As shown in Figure 13b,c, the serrated substances are observed in the micro-structures. When the wheat straw fibers are mixed, the strip substances are well occluded with the other hydration substrate, the contact surface is serrated, and there is no gap at the junction of the transition zone. However, many serrated substances are found in the SEM photos of specimens with rice straw and corn stalk, due to the fact that this type of fibers is prone to float on the surface of the matrix. Consequently, alkali-activated BFS with wheat straw fibers shows the optimum mechanical strengths.

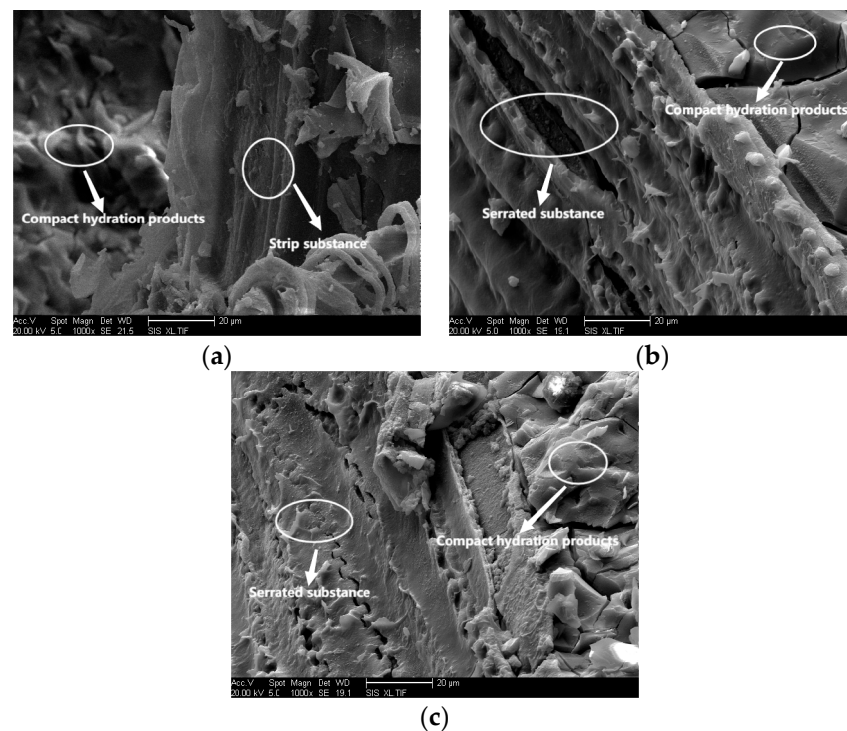


Figure 13. SEM of specimens. (a) With wheat straw; (b) With rice straw; (c) With corn stalk.

## 4. Conclusions

This study investigates the various influencing factors on the mechanical strengths of alkali-activated BFS powder. The research conclusions can be derived as follows.

Alkali-activated BFS powder with potassium silicate exhibits better mechanical strengths than the sodium silicate alkali-activated BFS powder. The flexural strengths of potassium silicate alkali-activated BFS cured for 3, 7, and 28 days are 3%, 24%, and 30.4% higher than those of the specimen mixed with sodium silicate. The compressive strengths of sodium silicate alkali-activated BFS cured for 3, 7, and 28 days are 4.4%, 3.3%, and 16.8%, respectively.

The modulus of alkali demonstrates a negative effect on the mechanical strengths of alkali-activated BFS powder. Alkali-activated BFS with 14% alkali shows the highest mechanical strengths. The flexural strength and compressive strength of the specimens with 14% alkali are 33.8% and 32.7% higher than those with 8% alkali. Meanwhile, the flexural strength and compressive strength of the specimens with 14% alkali are 21.2% and 17.1% higher than those with 18% alkali content.

The mechanical strengths of specimens with 35% water consumption are the highest, while specimens with 42% water consumption show the lowest mechanical strengths. The

flexural and compressive strengths of specimens with water consumption of 35% are 313% and 35.5% of the specimens with 42% water consumption.

An amount of 1% wheat straw fibers by volume of the total alkali-activated BFS powder and alkali treatment on fibers are the most favorable to the mechanical strength.

Strip substance has been found in the SEM photos of samples with wheat straw fibers, while the serrated substances are observed in the micro-structures of specimens with rice straw and corn stalk. The micro-structures of specimens with wheat straw fibers are the densest.

The alkali-activated BFS with the optimum mixing proportion and the manufacturing method can be applied in the repair of damaged buildings in the future. Nowadays, this kind of material is prone to cracking when applied in actual engineering. The rubber powder can be used to hinder the development of cracks. Such research will be conducted in the future.

**Author Contributions:** Conceptualization, J.Z., X.L. and H.W.; methodology, J.Z. and X.W.; validation, H.W. and L.S.; investigation, J.Z., H.W. and L.S.; data curation, X.L. and Z.Q.; writing—original draft preparation, J.Z.; writing—review and editing, Z.W.; supervision, H.W.; project administration, X.L. and Z.Q. All authors have read and agreed to the published version of the manuscript.

**Funding:** This research was sponsored by the Natural Science Foundation of Heilongjiang (LH2019E066), the Natural Science Foundation of China (51508140) and the Innovation and the College Students Innovation and Entrepreneurship Project (202110214006x, 202110214252). This support is hereby acknowledged.

**Institutional Review Board Statement:** Not applicable.

**Informed Consent Statement:** Not applicable.

**Data Availability Statement:** Not applicable.

**Conflicts of Interest:** The authors declare no conflict of interest.

## References

1. Poudyal, L.; Adhikari, K. Environmental sustainability in cement industry: An integrated approach for green and economical cement production. *Curr. Opin. Environ. Sustain.* **2021**, *4*, 100024. [\[CrossRef\]](#)
2. Provis, J.L.; Bernal, S.A. Geopolymers and related alkali-activated materials. *Adv. Mater. Res.* **2014**, *44*, 299–327. [\[CrossRef\]](#)
3. Jegan, M.; Annadurai, R.; Kannan Rajkumar, P.R. A state of the art on effect of alkali activator, precursor, and fibers on properties of geopolymer composites. *Constr. Mater.* **2023**, *18*, e01891. [\[CrossRef\]](#)
4. Van den Heede, P.; De Belie, N. Environmental impact and life cycle assessment (LCA) of traditional and ‘green’ concretes: Literature review and theoretical calculations. *Cem. Concr. Compos.* **2012**, *34*, 431–442. [\[CrossRef\]](#)
5. Bhutta, A.; Farooq, M.; Zanotti, C. Pull-out behavior of different fibers in geopolymer mortars: Effects of alkaline solution concentration and curing. *Mater. Struct.* **2017**, *50*, 80. [\[CrossRef\]](#)
6. Hasanbeigi, A.; Price, L.; Lin, E. Emerging energy-efficiency and CO<sub>2</sub> emission-reduction technologies for cement and concrete production: A technical review. *Renew. Sustain. Energy Rev.* **2012**, *16*, 6220–6238. [\[CrossRef\]](#)
7. Guo, Y.; Luo, L.; Liu, T.; Hao, L.; Li, Y.; Liu, P.; Zhu, T. A review of low-carbon technologies and projects for the global cement industry. *J. Environ. Sci.* **2024**, *136*, 682–697. [\[CrossRef\]](#)
8. Zhang, Z.; Zhang, J.; Yang, X.; Ning, Y.; Ji, T. Effect mechanism of slag activity on the basic tensile creep of alkali-activated slag mortar. *J. Build. Eng.* **2023**, *68*, 105903. [\[CrossRef\]](#)
9. Koppoju, M.; Mudimby, A.; Abhinay, A. Fracture parameters of flyash and GGBS based Alkali activated concrete. *Mater. Today* **2022**, *65*, 2053–2059. [\[CrossRef\]](#)
10. Mohanty, S.; Roy, N.; Singh, S.P.; Sihag, P. Strength and durability of flyash, GGBS and cement clinker stabilized dispersive soil. *Cold Reg. Sci. Technol.* **2021**, *191*, 103358. [\[CrossRef\]](#)
11. Varadharajan, S. Determination of mechanical properties and environmental impact due to inclusion of flyash and marble waste powder in concrete. *Structures* **2020**, *25*, 613–630. [\[CrossRef\]](#)
12. Nishanth, L.; Patil, N.N. Experimental evaluation on workability and strength characteristics of self-consolidating geopolymer concrete based on GGBFS, flyash and alccofine. *Mater. Today* **2022**, *59*, 51–57. [\[CrossRef\]](#)
13. Liu, H.; Wang, C.; Liu, X.; Wu, D.; Yang, H.; Zhang, Z.; Jan Khan, K.U. Deformation characteristics and prediction of unbound volcanic ash pavement based on the mechanistic-empirical design guide. *Constr. Build. Mater.* **2022**, *327*, 126975. [\[CrossRef\]](#)
14. Guler, S.; Akbulut, Z.F. Workability & mechanical properties of the single and hybrid basalt fiber reinforced volcanic ash-based cement mortars after freeze–thaw cycles. *Structures* **2023**, *48*, 1537–1547.

15. Liu, H.; Wang, C.; Wu, D.; Liu, X.; Zhang, Z. Deformation and critical dynamic stress for compacted volcanic ash subjected to monotonic and dynamic loads. *Constr. Build. Mater.* **2022**, *358*, 129454. [[CrossRef](#)]
16. Gobin, M.; Yasufuku, N.; Liu, G.; Watanabe, M.; Ishikura, R. Small strain stiffness, microstructure and other characteristics of an allophanic volcanic ash. *Eng. Geol.* **2023**, *313*, 106967. [[CrossRef](#)]
17. Zhang, H.; Ai, J.; Ren, Q.; Zhu, X.; He, B.; Jiang, Z. Understanding the strength evolution of alkali-activated slag pastes cured at subzero temperature. *Cem. Concr. Compos.* **2023**, *138*, 104993. [[CrossRef](#)]
18. Khaled, Z.; Mohsen, A.; Soltan, A.M.; Kohail, M. Optimization of kaolin into Metakaolin: Calcination Conditions, mix design and curing temperature to develop alkali activated binder. *Ain Shams Eng. J.* **2023**, *14*, 102142. [[CrossRef](#)]
19. Xu, Z.; Guo, Z.; Zhao, Y.; Li, S.; Luo, X.; Chen, G.; Liu, C.; Gao, J. Hydration of blended cement with high-volume slag and nano-silica. *J. Build. Eng.* **2023**, *64*, 105657. [[CrossRef](#)]
20. Jawad Ahmed, M.; Santos, W.F.; Brouwers, H.J.H. Air granulated basic Oxygen furnace (BOF) slag application as a binder: Effect on strength, volumetric stability, hydration study, and environmental risk. *Constr. Build. Mater.* **2023**, *367*, 130342. [[CrossRef](#)]
21. Yao, W.; Xia, K.; Liu, Y.; Shi, Y.; Peterson, K. Dependences of dynamic compressive and tensile strengths of four alkali-activated mortars on the loading rate and curing time. *Constr. Build. Mater.* **2019**, *202*, 891–903. [[CrossRef](#)]
22. Fang, S.; Shu Lam, E.S.; Li, B.; Wu, B. Effect of alkali contents, moduli and curing time on engineering properties of alkali activated slag. *Constr. Build. Mater.* **2020**, *249*, 118799. [[CrossRef](#)]
23. Zhang, S.; Niu, D. Hydration and mechanical properties of cement-steel slag system incorporating different activators. *Constr. Build. Mater.* **2023**, *363*, 129981. [[CrossRef](#)]
24. Shi, J.; Liu, B.; Chu, S.H.; Zhang, Y.; Zhang, Z.; Han, K. Recycling air-cooled blast furnace slag in fiber reinforced alkali-activated mortar. *Powder Technol.* **2022**, *407*, 117686. [[CrossRef](#)]
25. Chen, X.; Chen, J.; Li, M.; Wang, J.; Zhou, Z.; Du, P.; Zhang, X. Synthesis of kaliophilite from high calcium fly ash: Effect of alkali concentration. *Constr. Mater.* **2022**, *17*, e01542. [[CrossRef](#)]
26. Raj, R.S.; Arulraj, P.; Anand, N.; Kanagaraj, B.; Lubloy, E.; Naser, M.Z. Nanomaterials in geopolymer composites: A review. *Dev. Built Environ.* **2023**, *13*, 100114.
27. Tian, B.; Ma, W.; Li, X.; Jiang, D.; Zhang, C.; Xu, J.; He, C.; Niu, Y.; Dan, J. Effect of ceramic polishing waste on the properties of alkali-activated slag pastes: Shrinkage, hydration and mechanical property. *J. Build. Eng.* **2023**, *63*, 105448. [[CrossRef](#)]
28. Ionescu, B.A.; Barbu, A.-M.; Lăzărescu, A.-V.; Rada, S.; Gabor, T.; Florean, C. The Influence of Substitution of Fly Ash with Marble Dust or Blast Furnace Slag on the Properties of the Alkali-Activated Geopolymer Paste. *Coatings* **2023**, *13*, 403. [[CrossRef](#)]
29. Jamaludin, L.; Razak, R.A.; Al Bakri Abdullah, M.M.; Vizureanu, P.; Sandu, A.V.; Abd Rahim, S.Z.; Ahmad, R. Solid-to-Liquid Ratio Influenced on Adhesion Strength of Metakaolin Geopolymer Coating Paste Added Photocatalyst Materials. *Coatings* **2023**, *13*, 236. [[CrossRef](#)]
30. Cheng, H.; Chen, P.; Rong, X.; Cao, S.; Zhao, W. Effect of steel fibre and manufactured sand on mechanical properties of alkali-activated slag green cementitious material after high temperature. *Constr. Mater.* **2023**, *18*, e01919. [[CrossRef](#)]
31. Mastali, M.; Mohammad, S.K.; Abdollahnejad, Z. Towards sustainable bricks made with fiber-reinforced alkali-activated desulfurization slag mortars incorporating carbonated basic oxygen furnace aggregates. *Constr. Build. Mater.* **2020**, *232*, 117258. [[CrossRef](#)]
32. Santana, H.A.; Amorim Júnior, N.S.; Ribeiro, D.V.; Cilla, M.S.; Dias, M.R. Vegetable fibers behavior in geopolymers and alkali-activated cement based matrices: A review. *J. Build. Eng.* **2021**, *44*, 103291. [[CrossRef](#)]
33. Zhu, J.; Feng, S.; Liang, S. Experimental research on compressive performances of masonry after being subjected to high temperature. *Ind. Constr.* **2021**, *51*, 170–176.
34. Gao, K.; Cui, Y.; Zhang, P.; Zhao, T. Research Progress on Reinforcement Corrosion in Alkali Activated Concrete under Chloride Attack. *Bull. Chin. Ceram. Soc.* **2020**, *39*, 3070–3077.
35. Shi, J.; Guan, X.; Ming, J.; Zhou, X. Improved corrosion resistance of reinforcing steel in mortars containing red mud after long-term exposure to aggressive environments. *Cem. Concr. Compos.* **2022**, *130*, 104522. [[CrossRef](#)]
36. Vu, T.H.; Dang, L.C.; Kang, G.; Sirivivatnanon, V. Chloride induced corrosion of steel reinforcement in alkali activated slag concretes: A critical review. *Constr. Mater.* **2022**, *16*, e01112.
37. Feng, L.; Jin, K.; Wang, H. Research on the thermal conductivity and water resistance of foamed phosphogypsum. *Coatings* **2021**, *11*, 802. [[CrossRef](#)]
38. GB/T 17671-2021; Test Method of Cement Mortar Strength (ISO Method). The State Administration for Market Regulation: Beijing, China, 2021.
39. GB/T 17362-2008; Analysis Method for Gold Products with X-ray EDS in SEM. The Standardization Administration: Beijing, China, 2008.
40. Zhang, B.; Yu, T.; Deng, L.; Li, Y.; Guo, H.; Zhou, J.; Li, L.; Peng, Y. Ion-adsorption type rare earth tailings for preparation of alkali-based geopolymer with capacity for heavy metals immobilization. *Cem. Concr. Compos.* **2022**, *134*, 104768. [[CrossRef](#)]
41. Serdar, A.; Bulent, B. Effect of activator type and content on properties of alkali-activated slag mortars. *Ann. Compos.* **2014**, *57*, 166–172.
42. Shi, Z.; Shi, C.; Zhang, J.; Wan, S.; Zhang, Z.; Ou, Z. Alkali-silica reaction in waterglass-activated slag mortars incorporating fly ash and metakaolin. *Cem. Concr. Res.* **2018**, *108*, 10–19. [[CrossRef](#)]

43. Huang, W.; Wang, Y.; Zhang, Y.; Zheng, W. Experimental study of high-temperature resistance of alkali-activated slag crushed aggregate mortar. *Mater. Technol.* **2023**, *23*, 3961–3973. [[CrossRef](#)]
44. Ma, Q.; Yang, J.; Zhu, X.; Sreejith, V.; Huang, L. Influence of alkali concentration and modulus on compressive strength of alkali activated slag concrete. *New. Build. Mater.* **2019**, *46*, 1–4.
45. Shen, J.; Li, Y.; Lin, H.; Lv, J.; Feng, S.; Ci, J. Early properties and chemical structure analysis of alkali-activated brick geopolymer with varied alkali dosage. *J. Build. Eng.* **2022**, *60*, 105186. [[CrossRef](#)]
46. Zhang, S.; Ghoulah, Z.; Mucci, A.; Bahn, O.; Provençal, R.; Shao, Y. Production of cleaner high-strength cementing material using steel slag under elevated-temperature carbonation. *J. Cleaner Prod.* **2022**, *342*, 130948. [[CrossRef](#)]
47. Garanayak, L. Strength effect of alkali activated red mud slag cement in ambient condition. *Mater. Today* **2021**, *44*, 1437–1443. [[CrossRef](#)]
48. Wang, Q.; Sun, S.; Yao, G.; Wang, Z.; Lyu, X. Preparation and characterization of an alkali-activated cementitious material with blast-furnace slag, soda sludge, and industrial gypsum. *Constr. Build. Mater.* **2022**, *340*, 127735. [[CrossRef](#)]
49. Zhu, J.; Lesley, H.; Huang, Y.; Sun, Y. Experimental research on mechanical properties of different fibers reinforced alkali-activated slag cementitious material after high temperature. *J. Wuhan Univ. Technol.* **2020**, *44*, 97–102.
50. Tong, W.; Chu, Q.; Li, J.; Xie, X.; Wang, J.; Jin, Y.; Wu, S.; Hu, J.; Song, K. Insight into understanding sequential two-stage pretreatment on modifying lignin physiochemical properties and improving holistic utilization of renewable lignocellulose biomass. *Renew. Energy* **2022**, *187*, 123–134. [[CrossRef](#)]
51. Garlock, R.J.; Balan, V.; Dale, B.E. Comparative material balances around pretreatment technologies for the conversion of switchgrass to soluble sugars. *Bioresour. Technol.* **2011**, *102*, 11063–11071. [[CrossRef](#)]
52. Zhu, J.; Zheng, W.; Lessley, H. Mechanical properties of plant fibers reinforced alkali-activated slag cementitious material at hightemperature. *Ann. Chim. Sci. Mat.* **2019**, *43*, 240–255. [[CrossRef](#)]
53. Sellami, A.; Merzoud, M.; Amziane, S. Improvement of mechanical properties of green concrete by treatment of the vegetals fibers. *Constr. Build. Mater.* **2013**, *47*, 1117–1124. [[CrossRef](#)]

**Disclaimer/Publisher’s Note:** The statements, opinions and data contained in all publications are solely those of the individual author(s) and contributor(s) and not of MDPI and/or the editor(s). MDPI and/or the editor(s) disclaim responsibility for any injury to people or property resulting from any ideas, methods, instructions or products referred to in the content.